



# Adoption of low-carbon fuels reduces race/ethnicity disparities in air pollution exposure in California

Yiting Li <sup>a</sup>, Anikender Kumar <sup>b</sup>, Yin Li <sup>b</sup>, Michael J. Kleeman <sup>b,\*</sup>

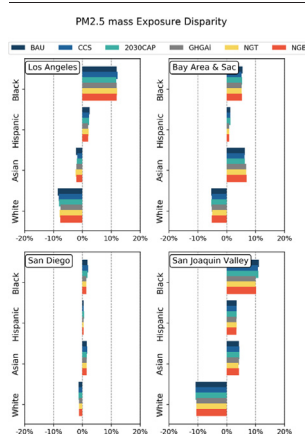
<sup>a</sup> Department of Land, Air, and Water Resources, University of California, Davis, United States of America

<sup>b</sup> Department of Civil and Environmental Engineering, University of California, Davis, United States of America

## HIGHLIGHTS

- Adoption of low carbon energy in 2050 reduces air pollution exposure in California.
- Black residents experience higher air pollution exposure than white residents.
- Adoption of low carbon energy reduces PM<sub>2.5</sub> exposure disparity by 20%.
- Adoption of low carbon energy reduces PM<sub>0.1</sub> exposure disparity by 40%.

## GRAPHICAL ABSTRACT



## ARTICLE INFO

Editor: Anastasia Paschalidou

### Keywords:

Low-carbon energy  
Air pollution  
Exposure disparity

## ABSTRACT

An environmental justice (EJ) analysis shows that adoption of low-carbon energy sources in the year 2050 reduces the race/ethnicity disparity in air pollution exposure in California by as much as 20% for PM<sub>2.5</sub> mass and by as much as 40% for PM<sub>0.1</sub> mass. An ensemble of six different energy scenarios constructed using the energy-economic optimization model CA-TIMES were evaluated in future years. Criteria pollutant emissions were developed for each energy scenario using the CA-REMARQUE model using 4 km spatial resolution over four major geographic areas in California: the greater San Francisco Bay Area including Sacramento (SFBA&SAC), the San Joaquin Valley (SJV), Los Angeles (LA), and San Diego (SD). The Weather Research & Forecasting (WRF) model was used to predict future meteorology fields by downscaling two different climate scenario (RCP4.5 and RCP8.5) generated by two different GCMs (the Community Climate System Model and the Canadian Earth Systems Model). Simulations were performed over 32 weeks randomly selected during the 10 year window from the year 2046 to 2055 to build up a long-term average in the presence of ENSO variability. The trends associated with low-carbon energy adoption were relatively stable across the ensemble of locations and scenarios. Deeper reductions in the carbon intensity of energy sources progressively reduced exposure to PM<sub>2.5</sub> mass and PM<sub>0.1</sub> mass for all California residents. The greater adoption of low-carbon fuels also reduced the racial disparity in the PM exposure. The three energy scenarios that achieved an ~80% reduction in GHG emissions relative to 1990 levels simultaneously produced the greatest reduction in PM exposure for all California residents and the greatest reduction in the racial disparity of that exposure. These findings suggest that the adoption of low-carbon energy can improve public health and reduce racial disparities through an improvement in air quality.

\* Corresponding author.

E-mail address: [mjkleeman@ucdavis.edu](mailto:mjkleeman@ucdavis.edu) (M.J. Kleeman).

## 1. Introduction

Exposure to atmospheric pollutants such as airborne particles with diameter less than 2.5  $\mu\text{m}$  ( $\text{PM}_{2.5}$ ) is estimated to cause 3.3 million premature deaths per year worldwide (Lelieveld et al., 2015). The majority of this excess mortality occurs in heavily populated regions of Asia, but even cleaner regions in North America and Europe experience a public health burden associated with air pollution (Organization, 2021; Strak et al., 2021). Numerous environmental justice (EJ) studies have shown that lower socio-economic classes in the United States experience higher levels of air pollution, which subjects them to a lifetime of health risk (Anderson et al., 2018; Bravo et al., 2016; Colmer et al., 2020; Cushing et al., 2015; Liu et al., 2021; Miranda et al., 2011; Tessum et al., 2021; Thakrar et al., 2020). This exposure disparity can come from many different sources of air pollution, including transportation (Günier et al., 2003; Houston et al., 2014; Rowangould, 2013), food cooking (Shah et al., 2020), residential combustion (Tessum et al., 2019), electricity (Thind et al., 2019) and industrial facilities (Perlin et al., 2002). Exposure to poor air quality at any stage of life is associated with a variety of health problems that burden our collective health care system and reduces our economic output. A sustainable future in an increasingly globalized and competitive world requires that we minimize costs for avoidable illness to help all people reach their full potential regardless of their socio-economic class.

Energy consumption across the economy is inherently associated with air pollution, linking the issues of climate change and air quality. A recent study suggests that global air pollution mortality could double by the year 2050 under a business-as-usual (BAU) energy scenario (Lelieveld et al., 2015). Many previous studies have estimated health co-benefits of various GHG reduction pathways, including adopting carbon capture and sequestration (CCS) technology, limiting bioenergy, using renewable energy in electricity generation, and reducing fossil fuels in power plants (Dimanchev et al., 2019; Markandya et al., 2018; Ramaswami et al., 2017; Sampedro et al., 2020; Wang et al., 2020; West et al., 2017; Zapata et al., 2018b). Global reductions in GHG emissions have been estimated to reduce premature mortality by 17%–23%. The health co-benefits in many scenarios exceed the mitigation costs. India and China obtain greater co-benefits than other countries (Markandya et al., 2018; Sampedro et al., 2020), but impressive life-saving and health co-benefits were also demonstrated in the US by adopting the United States (US) Clean Power Plan (Driscoll et al., 2015; Levy et al., 2016), sub-national renewable energy policies (Dimanchev et al., 2019) and multi-sector GHG mitigation pathway (Zhang et al., 2016, 2017). However, these same studies also concluded that air quality improvements and health co-benefits varied significantly by region, suggesting that location-specific analyses may be warranted.

California is the most populous state/province in North America, has the largest sub-national economy in the world, and is home to six out of the ten most polluted cities in the US based on annual-average  $\text{PM}_{2.5}$  concentrations (American Lung Association, 2019). California is leading North America in the adoption of new sustainable energy sources to mitigate climate change. State law AB32 commits California to reduce GHG emissions to 1990 levels by 2020 (California Air Resource Board, 2006); California Governor's Executive Order S-3-05 commits California to an additional 80% reduction by 2050 (Gov Arnold Schwarzenegger, 2005). This massive reduction in GHG emissions will require a transformation in the energy system that will involve choices about technological, fuel and energy resources. All of these choices will fundamentally change the patterns of air pollution exposure in California. Multiple previous studies have evaluated the health co-benefits that can be achieved under various GHG mitigation pathways (Kleeman et al., 2013; Wang et al., 2020; Zapata et al., 2018b; Zhao et al., 2019), but very few studies have explicitly explored the intersection of GHG emissions reductions, air pollution exposures, and racial disparities in exposure.

Here we conduct a comprehensive analysis of health co-benefits, racial disparities, and source/composition in air pollution exposure under six future energy scenarios and four future meteorology scenarios in California. Air pollution exposure is calculated for four racial groups defined by the American Community Survey (ACS): Black, Hispanic, Asian, and White (United State Census Bureau, 2020). Public health benefits associated with reduced air pollution in different energy scenarios are calculated using standard epidemiological relationships (US EPA, 2021). Energy scenarios are identified that reduce the racial disparity in air pollution exposure and total population exposure. The most promising strategies/emissions sources to reduce future racial disparities/total population exposure to air pollution are then discussed.

## 2. Methodology

### 2.1. Energy scenarios

Future energy scenarios for California are described in detail by Li et al. (2022) and so only a brief summary is presented in here. All energy scenarios were created using the CA-TIMES energy economic model (McCollum et al., 2012; Yang et al., 2015) that predicts the statewide least-cost technology mix across all energy sectors in California to achieve target GHG reductions subject to external policy constraints. Three energy scenarios achieved the objective of an 80% reduction in GHG emissions relative to 1990 levels, while the remaining scenarios achieved lower reductions. Table 1 summarizes the major features of each energy scenario.

Criteria pollutant emissions with 4 km spatial resolution associated with each energy scenario were calculated with the CA-REMARQUE model (Li et al., 2022). CA-REMARQUE applies tailored procedures for each energy sector in California to estimate how the adoption of low-carbon fuels will modify criteria pollutant emissions. Emissions from the production and combustion of bio-fuels incorporate the latest measurement data available in the literature.

### 2.2. Meteorological scenarios

Meteorological scenarios were produced using the Weather Research and Forecast (WRF) model v3.4 (NACR, 2012) based on initial and boundary conditions predicted by the Community Climate System Model (CCSM) (Gent et al., 2011) and the Canadian Earth Systems Model (CanESM) (Swart et al., 2019). The global climate scenarios associated with Representative Concentration Pathway 4.5 (RCP4.5)

**Table 1**  
Energy scenarios descriptions.

Scenario name	Description
BAU	A business-as-usual scenario that includes current regulations and future growth projections.
GHGAI	A strict GHG reduction scenario that achieves 80% reduction of GHG emission (relative to 1990 levels) by the year 2050. More than 60% of California's primary energy supplied by renewables including biomass, wind, and solar.
2030CAP	A loose GHG reduction scenario that meets current policy references but only achieves a 40% GHG reduction by the year 2030 with no further reductions thereafter.
CCS	A scenario that allows for more combustion to generate electricity by focusing on adoption of carbon capture and sequestration technology. Meets the 80% GHG reduction target by counting "negative emissions" from carbon capture technology.
NGB	A variation of the GHGAI scenario that allows for 20% more natural gas combustion for residential and commercial buildings.
NGT	A variation of the GHGAI scenario that allows for 20% more natural gas combustion for electricity generation

and RCP8.5 were selected for both CCSM and CanESM, yielding four different meteorological scenarios. Thirty vertical layers were used in the WRF model up to a top height of approximately 15 km. The maximum spatial resolution of the results used in the present analysis was 4 km. Thirty-two weeks were randomly selected for study across the ten-year window from 2046 to 2055. Sensitivity analysis indicates that the average air pollution concentrations predicted over this thirty-two week sample captures the long-term average concentrations with a standard error of  $0.23 \mu\text{g m}^{-3}$  in the presence of the El Nino Southern Oscillation (ENSO).

### 2.3. Air quality simulations

Air quality simulations were performed using the UCD/CIT chemical transport model (Kleeman and Cass, 2001; Ying et al., 2007). Three nested domains were used to cover all of California at 24 km resolution, Southern California at 4 km resolution, and Central/Northern California with 4 km resolution. Fifteen telescoping vertical levels were used up to a total height of 5 km with the first ten levels in the lowest 1 km of the atmosphere. Numerous previous studies have demonstrated the suitability of this model configuration when simulating historical pollution events in California (Hu et al., 2014, 2015, 2017; Laurent et al., 2014; Li et al., 2020; Mahmud et al., 2012; Ostro et al., 2015).

All simulations used the SAPRC11 chemical mechanism to predict oxidant concentrations and the formation of photochemical products including ozone ( $\text{O}_3$ ), acids such as nitric acid ( $\text{HNO}_3$ ), and semi-volatile organic species. The condensation of inorganic salts such as ammonium nitrate ( $\text{NH}_4\text{NO}_3$ ) was predicted using the ISSORPIA thermodynamic routine (Fountoukis and Nenes, 2007) coupled with the APCD gas-particle partitioning scheme (Jacobson, 2010). The formation of secondary organic aerosol (SOA) was simulated using an n-product model tuned to account for vapor wall losses during smog chamber experiments (Cappa et al., 2016). The ability of the modeling system to accurately predict  $\text{PM}_{2.5}$ ,  $\text{PM}_{0.1}$ , and particle number concentrations at locations across California is described in detail by Yu et al. (2019).

### 2.4. Socio-economic data

Socio-economic data from the American Community Survey (ACS) 2012–2016 (United State Census Bureau, 2020) was used to calculate air pollution exposure for different race/ethnicity groups in California. The ACS dataset includes race/ethnicity information for Black (Black & African American alone), Hispanic (Hispanic or Latino, regardless of race), Asian (Asian alone), and non-Hispanic White (White, not

Hispanic or Latino) at the census tract level. The future EJ analysis focuses on four geographic regions across California: (i) Los Angeles (LA), (ii) San Diego (SD), (iii) San Joaquin Valley (SJV), and (iv) the San Francisco Bay Area & Sacramento (SFBA & SAC). The population densities of each race within each of these geographic regions are shown in Figs. S1–S10. These four regions include more than 90% of California's population, making the EJ analysis in current study representative of the entire state.

Table 2 shows the race/ethnicity composition of the population in each geographic region analyzed in the current study. Black & African American residents account for 4–6% of the total population in each region, Asian residents account for 6–20% of the total population, White residents account for 30–48% of the total population, and Hispanic residents account for 26–54% of the total population. Figs. S1–S10 show that some race/ethnicity groups are clustered in sub-regions of each domain. Specifically, Black & African American residents are clustered into neighborhoods south of central Los Angeles, and Asian residents are clustered into neighborhoods in Oakland. These clustering effects have a significant impact on the air pollution exposure for race/ethnicity groups.

### 2.5. Population exposure, environmental justice, and health co-benefits calculations

$\text{PM}_{2.5}$  and  $\text{PM}_{0.1}$  population weighted concentrations (PWC) were calculated for total population and each race/ethnicity group under an ensemble of six energy scenarios and four meteorological scenarios in four sub-regions in California. Absolute/relative exposure and absolute disparity by race/ethnicity were analyzed to show the ability of each scenario i) to reduce air pollutants exposure for all residents; and ii) to mitigate the exposure disparity between races/ethnicities. Results are shown in Sections 3.1 and 3.2.

The health co-benefits of  $\text{PM}_{2.5}$  and  $\text{PM}_{0.1}$  within each member of the ensemble was calculated using the Environmental Benefits Mapping and Analysis Program – Community Edition (BenMap-CE) v1.4.8 developed by US EPA (US EPA, 2021). The BAU scenario was used as a baseline and the GHGAi, 2030CAP, CCS, NGB and NGT were used as controls in the BenMap analysis. Four health impact functions were analyzed, including Krewski et al. (2009), Laden et al. (2006), Lepeule et al. (2012) and Pope et al. (2002). Economic benefits were then calculated with the value of a statistical life (VSL) of \$7.6 M. Results are shown in Section 3.3.

Emissions source contributions to  $\text{PM}_{2.5}/\text{PM}_{0.1}$  exposure were analyzed for each scenario, race/ethnicity, and region. Nine emissions source sectors were used in this study, including i) tire & brake

**Table 2**  
Socio-economic data summary.

Region	Population				Percentage			
	LA <sup>a</sup>	SFBA & SAC <sup>b</sup>	SJV <sup>c</sup>	SD <sup>d</sup>	LA	SFBA & SAC	SJV	SD
All	14,384,814	11,299,258	2,526,861	2,967,636				
Black <sup>e</sup>	920,808	674,400	99,250	146,401	6.40%	5.97%	3.93%	4.93%
Hispanic <sup>f</sup>	6,690,133	2,921,051	1,364,228	934,465	46.51%	25.85%	53.99%	31.49%
Asian <sup>g</sup>	2,141,542	2,287,506	159,652	357,288	14.89%	20.24%	6.32%	12.04%
White <sup>h</sup>	4,270,607	4,901,766	853,299	1,420,956	29.69%	43.38%	33.77%	47.88%

<sup>a</sup> Los Angeles.

<sup>b</sup> San Francisco Bay Area & Sacramento.

<sup>c</sup> San Joaquin Valley.

<sup>d</sup> San Diego.

<sup>e</sup> Black and African American.

<sup>f</sup> Hispanic or Latino, regardless of races.

<sup>g</sup> Asian Alone.

<sup>h</sup> Non-Hispanic White.

wear; ii) on-road mobile tailpipe; iii) off-road equipment; iv) aircraft & marine vessels; v) residential & food cooking; vi) electricity generation; vii) fuel supply that depends on the energy scenario; viii) fuel supply that doesn't change with scenarios; and ix) biomass burning & construction dust (wildfires were excluded due to inherent uncertainty about location and timing). Further details of the emissions patterns associated with each sector under each scenario are discussed by Li et al. (2022). Results are shown in Section 3.4. The further investigation of impacts of each source contribution to total PWC and EJ are presented in Section 3.5.

### 3. Results

#### 3.1. Absolute exposure

Fig. 1 shows population-weighted concentrations (PWC) for  $PM_{0.1}$  and  $PM_{2.5}$  mass in four different California regions: Los Angeles, San Diego, the Bay Area & Sacramento, and the San Joaquin Valley. Results for individual race/ethnicity groups and for the average across all groups are shown for each energy scenario. All exposure concentrations were averaged across the four meteorology scenarios, with uncertainty bars shown to represent one standard deviation between the meteorological scenarios. Meteorological variability influences  $PM_{0.1}$  and  $PM_{2.5}$  mass concentrations but does not significantly affect comparisons between different energy scenarios. The absolute exposure concentrations for individual meteorological scenarios are provided in Figs. S11–S18.

Both  $PM_{2.5}$  and  $PM_{0.1}$  absolute exposure concentrations vary across regions. The highest  $PM_{2.5}$  and  $PM_{0.1}$  concentrations are predicted to occur in Los Angeles, followed by the San Joaquin Valley, with lower absolute exposure concentrations predicted in San Diego and the Bay Area & Sacramento. Averaged across all energy scenarios,  $PM_{2.5}$  absolute exposure ranges from

8.2  $\mu\text{g}/\text{m}^3$  to 12.5  $\mu\text{g}/\text{m}^3$ ,  $PM_{0.1}$  absolute exposure ranges from 1.3  $\mu\text{g}/\text{m}^3$  to 2.2  $\mu\text{g}/\text{m}^3$ .

The choice of future energy scenario influences the absolute PWC for  $PM_{2.5}$  and  $PM_{0.1}$ . Absolute PWCs of both  $PM_{2.5}$  and  $PM_{0.1}$  are highest in the BAU scenario and lowest in the GHGAI scenario for all regions. The  $PM_{2.5}$  exposure concentrations in the CCS and 2030CAP scenarios are only slightly lower than the concentrations in the BAU scenario. The  $PM_{2.5}$  exposure concentrations in the NGT and NGB scenarios are slightly higher than the concentrations in the GHGAI scenario.

$PM_{0.1}$  exposure concentrations are more variable than  $PM_{2.5}$  exposure concentrations on a relative scale across energy scenarios and geographical regions. For example, NGT produces 8.2%/5.5% higher  $PM_{0.1}$  exposure than GHGAI/NGB in Los Angeles, but the corresponding relative increase in  $PM_{2.5}$  concentrations is only 2.3%/1.6%. In the San Francisco Bay Area and Sacramento, NGB increases  $PM_{0.1}$  exposure by 12%/10% compared to GHGAI/NGT, but corresponding increases to  $PM_{2.5}$  exposure are only 2.7%/2.5%. Thus, relative changes to  $PM_{0.1}$  concentrations across energy scenarios can be as much as four times greater than relative changes to  $PM_{2.5}$  concentrations. These results once again reflect the greater variability of  $PM_{0.1}$  emissions than  $PM_{2.5}$  emissions across different energy scenarios (Li et al., 2022; Zapata et al., 2018a).

Absolute exposure disparities are commonly used to quantify the severity of an environmental justice problem (Clark et al., 2017; Harper et al., 2013; Liu et al., 2021; Paoletta et al., 2018). Absolute exposure disparities between race/ethnicity groups were calculated as the difference between the group with the highest exposure concentration (minority) and the group with the lowest exposure concentrations. The lowest exposure group was consistently White residents in this study. Exposure disparities for  $PM_{2.5}$  concentrations exist in all geographical regions within California, with the maximum value

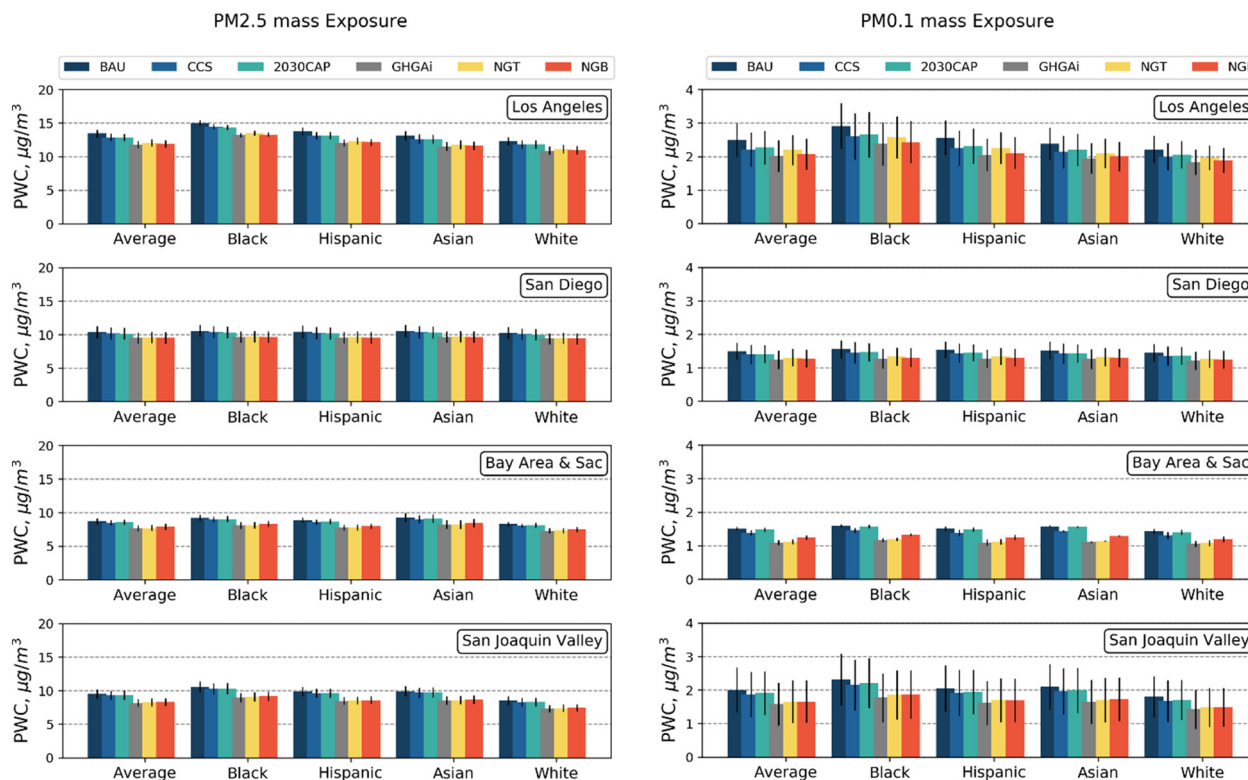


Fig. 1. Future year (2050)  $PM_{2.5}$  (left) and  $PM_{0.1}$  (right) Population Weighted Concentrations (PWC) by energy scenario and race/ethnicity across four regions in California. Each bar and associated uncertainty range represents the average and standard deviation across four meteorological scenarios (CCSM8.5, CCSM4.5, CAN8.5, CAN4.5).

predicted in Los Angeles and the minimum value predicted in San Diego (see Fig. 2). Locations with high exposure disparity have neighborhoods dominated by one race/ethnicity group with air pollution concentrations that are significantly different from regional average concentrations.

Trends in absolute exposure disparities across energy scenarios are similar to the trends in the underlying  $PM_{2.5}$  and  $PM_{0.1}$  absolute exposure concentrations. None of the clean fuel energy scenarios can eliminate environmental disparity in the future year 2050, but adoption of low-carbon energy sources in the year 2050 reduces the race/ethnicity disparity in air pollution exposure in California by as much as 20% for  $PM_{2.5}$  mass and by as much as 40% for  $PM_{0.1}$  mass (see Fig. 2). Deeper reductions in the carbon intensity of energy sources progressively reduced exposure to  $PM_{2.5}$  mass and  $PM_{0.1}$  mass for all California residents. The greater adoption of low-carbon fuels also reduced the race/ethnicity disparity in the PM exposure. The three energy scenarios that achieved an ~80% reduction in GHG emissions relative to 1990 levels (GHGAi, NGB, NGT) simultaneously produced the greatest reduction in PM exposure for all California residents and the greatest reduction in the race/ethnicity disparity of that exposure. The energy scenarios that allow continued use of combustion to generate a substantial fraction of California's energy demand (2030CAP, CCS) typically produce less than half of the reduction in absolute exposure disparities.

### 3.2. Relative exposure

Fig. 3 shows the  $PM_{2.5}$  and  $PM_{0.1}$  exposure disparity (relative to average exposure) for Black & African American, Hispanic, Asian, and non-Hispanic White residents in different geographic regions within California. Results are averaged across all meteorological scenarios but shown individually for all energy scenarios. Details of each meteorology scenario are shown in Figs. S19–S26. Relative exposure disparities greater than zero indicate that the race/ethnicity group has

greater-than-average exposure, while relative exposure disparities less than zero indicate that the race/ethnicity group has less-than-average exposure. Black & African American residents experienced higher-than-average exposure to  $PM_{2.5}$  and  $PM_{0.1}$  in all future energy scenarios in all study regions (Los Angeles, San Francisco, Sacramento, San Diego, and the San Joaquin Valley). Asian residents in San Francisco experienced higher-than-average exposure to air pollution in all future energy scenarios. Peak exposure disparities reached ~10% for  $PM_{2.5}$  and ~20% for  $PM_{0.1}$ . White residents experience lower-than-average exposures in all regions, with peak disparity values of approximately -10% for both  $PM_{2.5}$  and  $PM_{0.1}$ . Hispanic residents generally experience exposure concentrations that are close to average. Asian residents experience lower-than-average  $PM_{2.5}$  exposure concentrations in Los Angeles but higher-than-average exposure concentrations in the San Francisco Bay Area and Sacramento.

The results summarized in Fig. 3 reflect the spatial distribution of each race/ethnicity group within each geographic region. Black & African American residents in California are clustered into neighborhoods near the center of urban cores or near major transportation corridors where air pollution emissions are higher. The historical policies that have produced these housing patterns are beyond the scope of the current study, but interested readers are referred to studies on the effects of “redlining” (see for example (Nardone et al., 2020; Zenou and Boccard, 2000)). Due to their proximity to higher emissions, Black & African American residents often experience higher-than-average exposure concentrations. White residents are more dispersed in suburban neighborhoods that are further away from urban cores. This housing pattern leads to lower-than-average exposure for White residents. Asian residents are clustered near urban cores in Northern California (such as downtown San Francisco, San Jose, etc.) leading to higher-than-average exposure concentrations. Asian residents are dispersed in suburban neighborhoods in Southern California, leading to lower-than-average exposure concentrations in this sub-region. The contrast between exposure concentrations for Asian residents living in Northern

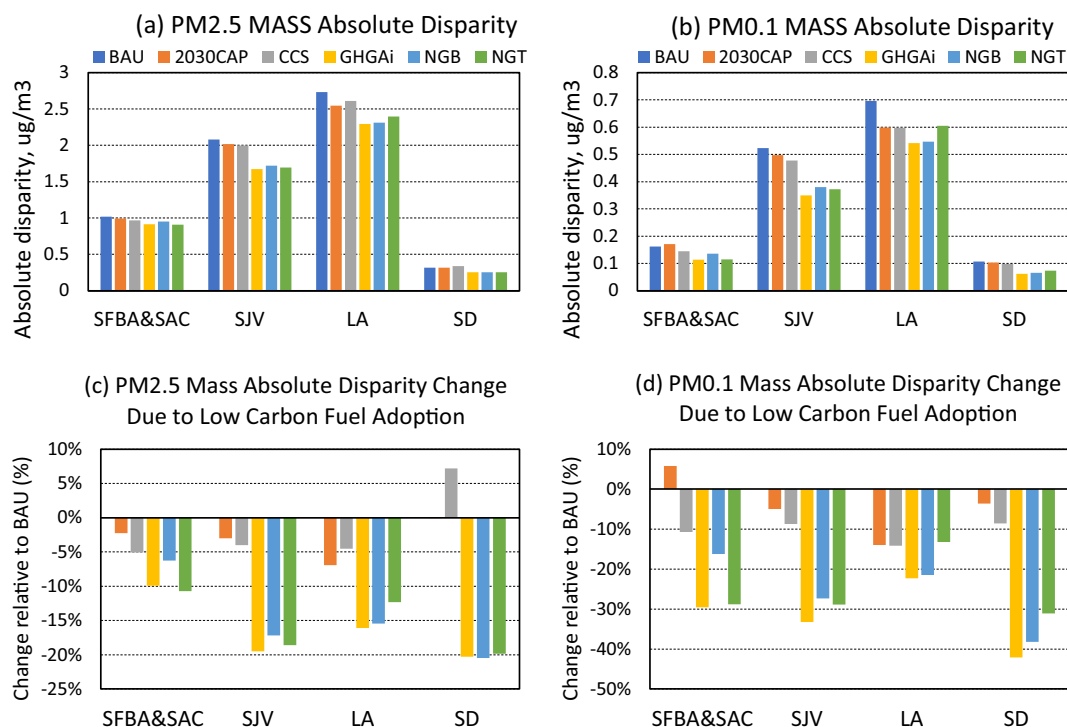
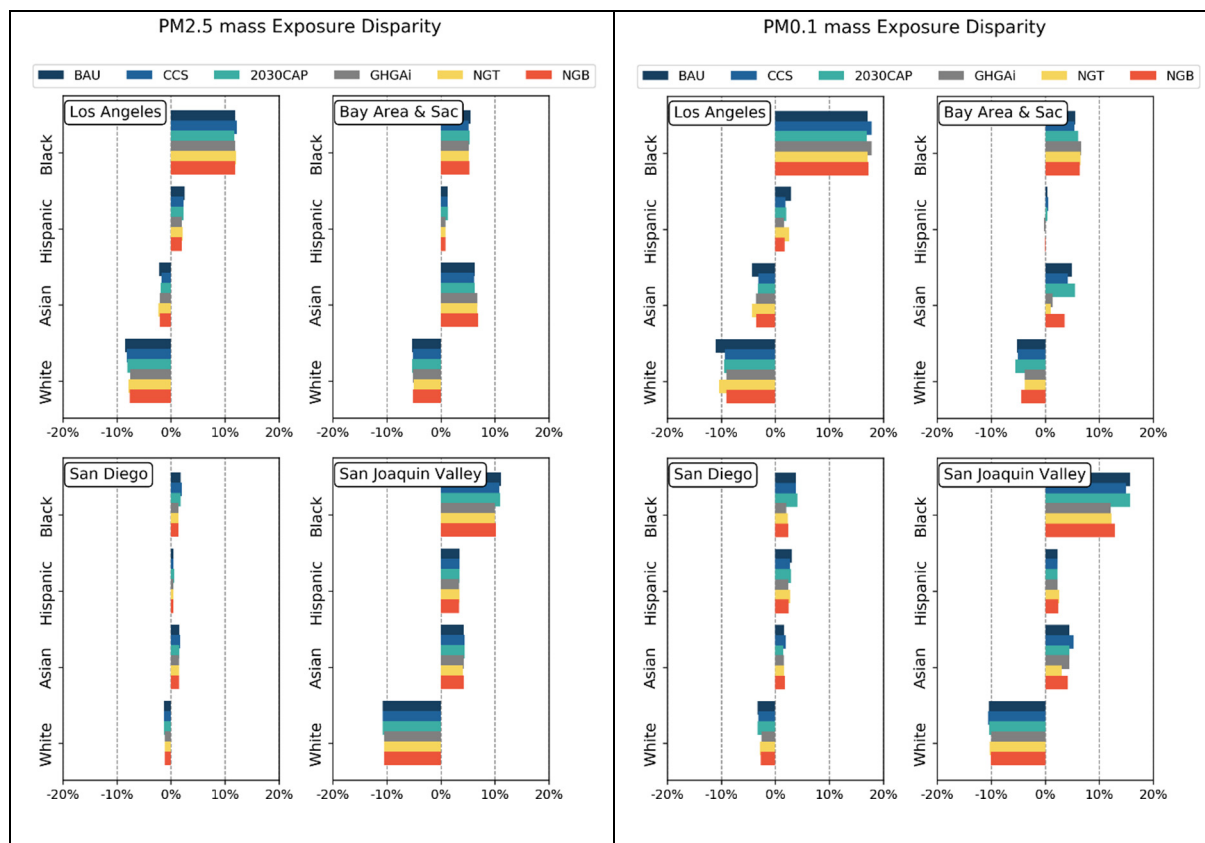


Fig. 2. Change in  $PM_{2.5}$  mass and  $PM_{0.1}$  mass absolute exposure disparities under different future energy scenarios. Absolute exposure disparities between race/ethnicity groups were calculated as the difference between the group with the highest exposure concentration and the group with the lowest exposure concentrations. Top panels show absolute values of population-weighted concentrations, while bottom panels show changes relative to the BAU scenario.



**Fig. 3.** Future year (2050)  $PM_{2.5}$  mass (left) and  $PM_{0.1}$  mass (right) exposure disparity (relative to total population) by scenario and race/ethnicity across four regions in California. Each bar represents the average across four meteorological scenarios (CCSM8.5, CCSM4.5, CAN8.5, CAN4.5).

California vs. Southern California emphasizes the importance of the distance between the home address and the urban core when calculating exposure concentrations.

### 3.3. Health co-benefits

Fig. 4 quantifies the avoided mortality and public health benefits associated with each energy scenario. Health benefits per 1 M residents are similar for Asian and Black & African American residents, slightly lower for Hispanic residents, and slightly higher for White residents (see right panel Fig. 4). These patterns reflect the spatial distribution of the population comprising each racial group relative to the average air pollution exposure fields. Total health benefits for each racial category expressed as avoided mortality and public health savings (billions of USD) are calculated by multiplying average health benefits by total population (see left panel of Fig. 4). Energy scenarios with deeper cuts to GHG emissions produce greater public health benefits for all racial categories.

### 3.4. Source contributions

Figs. 5 and 6 show predicted exposure to primary sources of  $PM_{2.5}$  and  $PM_{0.1}$  for different race/ethnicity groups in Los Angeles under the six different energy scenarios. The X-axis in Figs. 5 and 6 represents the primary contribution from each source to the total PM exposure. Similar plots for other geographic regions are shown in Figs. S27–S32. All results are based on the average of the four meteorological scenarios since trends within each meteorological scenario were consistent.

Different sources dominate exposure to  $PM_{2.5}$  vs.  $PM_{0.1}$ . Tire & brake wear, residential & cooking, unchanged fuel supply, and construction dust are the major sources for  $PM_{2.5}$ . Emissions from these sources generally do not change significantly between energy scenarios, and so the

predicted  $PM_{2.5}$  source contributions are relatively constant across Fig. 5. Off-road equipment, residential & cooking, electricity generation, and unchanged fuel supply are the major sources of  $PM_{0.1}$  exposure. The fuels used for off-road equipment and electricity generation change significantly between energy scenarios, and so there is significant variability in  $PM_{0.1}$  source contributions illustrated in Fig. 6.  $PM_{0.1}$  concentrations are dominated by primary emissions (Hu et al., 2014) leading to sharper spatial gradients (Karner et al., 2010).  $PM_{0.1}$  concentrations are therefore influenced by local emissions to a larger degree than  $PM_{2.5}$  concentrations, making the spatial distribution of each race/ethnicity group more important when determining exposure concentrations.

It is noteworthy that residential & cooking emissions are a dominant source for both  $PM_{2.5}$  and  $PM_{0.1}$ . These emissions are related to human activities, and they are located close to residences, leading to higher intake fractions (Evans et al., 2002; Marshall et al., 2003, 2005). Targeted reductions for residential & cooking sources could be used to reduce future PM concentrations.

### 3.5. Potential for further improvements

The GHGAI scenario improves public health, but it does not completely eliminate race/ethnicity disparity in exposure to air pollution in California. The detailed source apportionment information embedded in the UCD/CIT model can be analyzed to identify additional measures to further reduce disparity. This analysis will use the GHGAI scenario as the most promising starting point for further improvements.

#### 3.5.1. Improvements for total population exposure

Fig. 7 illustrates the efficiency of  $PM_{2.5}$  emissions reductions in the GHGAI scenario quantified as the change in total exposure

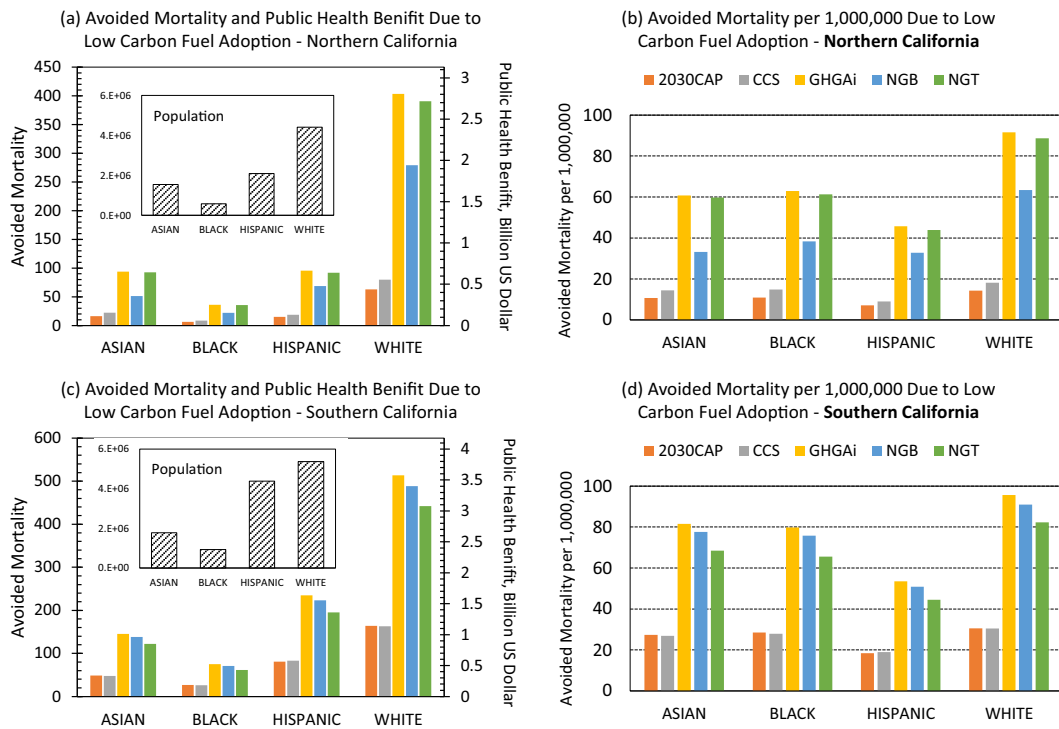


**Fig. 4.** Avoided mortality and public health benefits associated with low-carbon energy scenarios (relative to the BAU scenario) in Northern California (SFBA&SAC, SJV) and Southern California (LA, SD). Public health benefits calculated using Value of a Statistical Life (VSL) estimated to be \$7.6M in the year 2050.

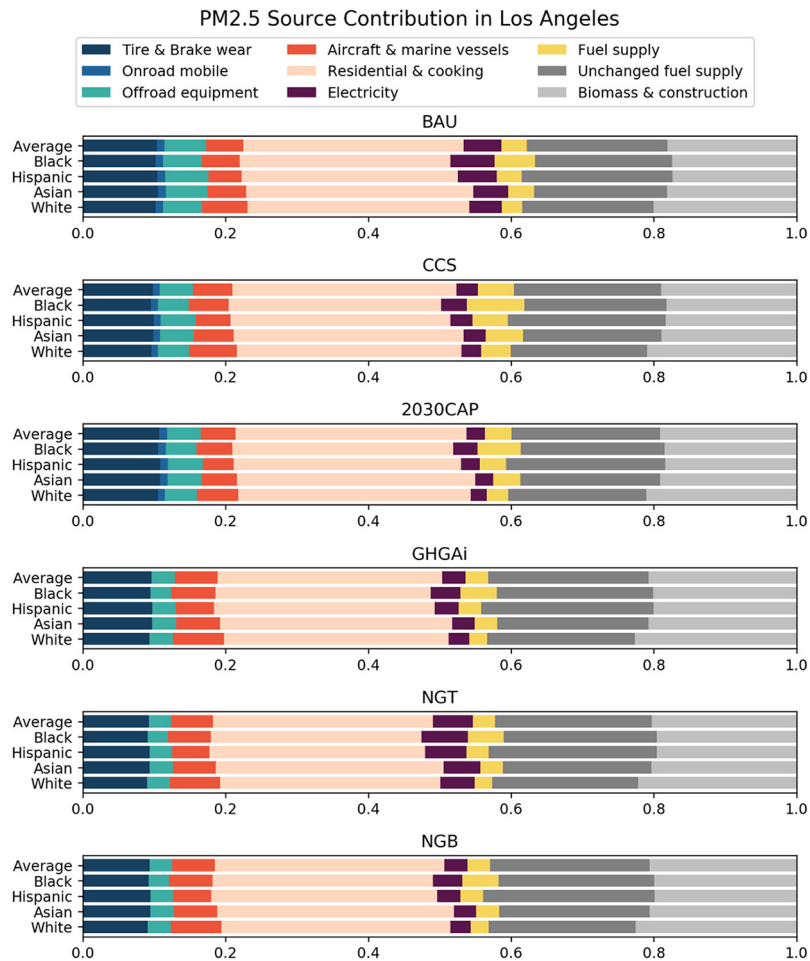


**Fig. 5.** PM<sub>2.5</sub> source contributions in Los Angeles area by energy scenarios and race/ethnicity. Each value represents the average across four meteorological scenarios.

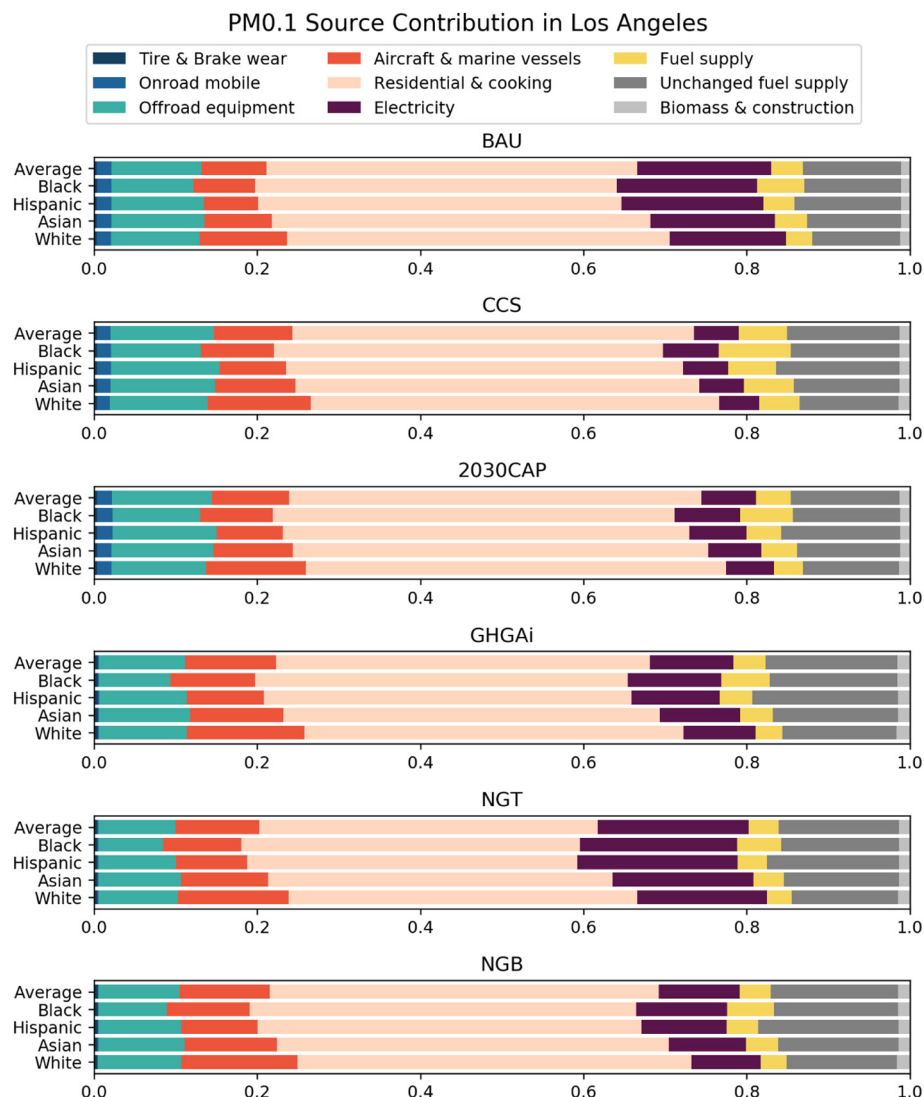


Fig. 6. PM<sub>0.1</sub> source contributions in Los Angeles area by energy scenarios and race/ethnicity. Each value represents the average across four meteorological scenarios.

concentrations (without regard for race/ethnicity). Similar plots for other energy scenarios shown in Figs. S33–S36. The horizontal axis of each subpanel in Fig. 7 indicates the amount of emissions reductions in the GHGAI scenario relative to the BAU scenario for each of the indicated source categories. The vertical axis of each subpanel indicates the corresponding change in population-weighted concentration. The position of each symbol in Fig. 7 reflects the intake fraction of the source emissions determined by the emissions location relative to the population. The size of the symbol in Fig. 7 is proportional to the amount of PM<sub>2.5</sub> emissions associated with the indicated source category. Emissions from residential and food cooking sources are large, have high intake fraction, and they have been reduced by only a modest amount in the GHGAI scenario. Further reductions in emissions from residential and food cooking sources could significantly reduce PM<sub>2.5</sub> exposure in the future years.

PM<sub>2.5</sub> tailpipe emissions from on-road mobile sources undergo the greatest relative reduction in the GHGAI scenario, but the corresponding absolute reduction in population-weighted concentration is modest because tailpipe emissions from motor vehicles were already quite low in the BAU scenario due to the adoption of advanced emissions control technology. The near-total elimination of tailpipe emissions from motor vehicles achieved by converting the majority of the light-duty vehicle fleet to non-combustion power therefore has modest benefits for public health in the GHGAI scenario. It is noteworthy that tire and brake-wear emissions

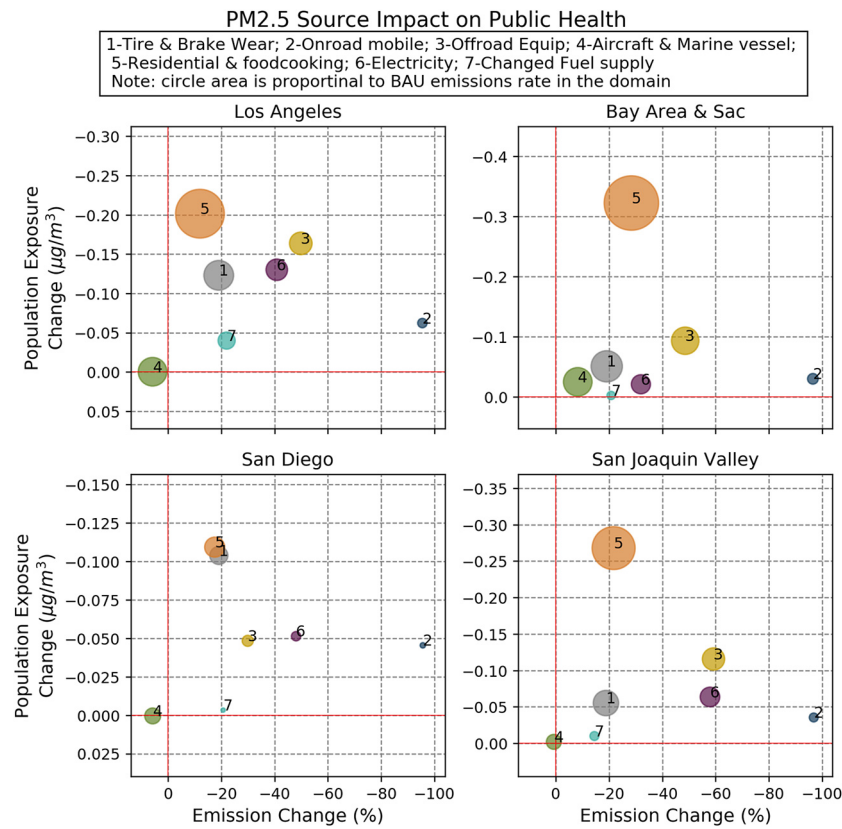
from mobile sources are significantly greater than tailpipe emissions in the GHGAI scenario. Further reductions from mobile sources should focus on reduced dust from braking systems (Cai et al., 2019; Gramstat, 2018) and development of new tire compounds (Dalmau et al., 2020; Fonseca et al., 2020; Panko et al., 2018) in order to further reduced PM<sub>2.5</sub> exposure.

Fig. 8 illustrates the efficiency of PM<sub>0.1</sub> emissions reductions using the same format as Fig. 7. Results for other energy scenarios are shown in Figs. S37–S40. Large residential and cooking emissions are once again identified as a category that has high PM<sub>0.1</sub> intake fraction and that has undergone only partial emissions controls in the GHGAI energy scenario. Electricity generation is the next most promising source of PM<sub>0.1</sub> emissions reduction, but the GHGAI scenario already controls these emissions by >50% and the intake fraction is relatively low because most electricity generation stations are located far from major population centers.

Based on Figs. 7 and 8, aircraft emissions have the lowest relative reduction in both PM<sub>2.5</sub> and PM<sub>0.1</sub> emissions in the GHGAI scenario, suggesting that this category could be targeted for further reductions. Such measures would reduce primary PM<sub>2.5</sub>/PM<sub>0.1</sub> (shown in Figs. 7 + 8) and nucleated ultrafine particles (not shown) (Yu et al., 2019).

### 3.5.2. Improvements to reduce disparity across race/ethnicity

Reducing PM<sub>2.5</sub> exposure disparities across race/ethnicity requires that emissions reductions be prioritized for source categories that



**Fig. 7.** PM<sub>2.5</sub> source impact on public health (regardless of race) for GHGAI energy scenario. X-axis indicates emissions (source) changes between BAU and GHGAI scenario. Y-axis indicates PWC changes between BAU and GHGAI scenario for specific source. All results averaged across four meteorological scenarios.

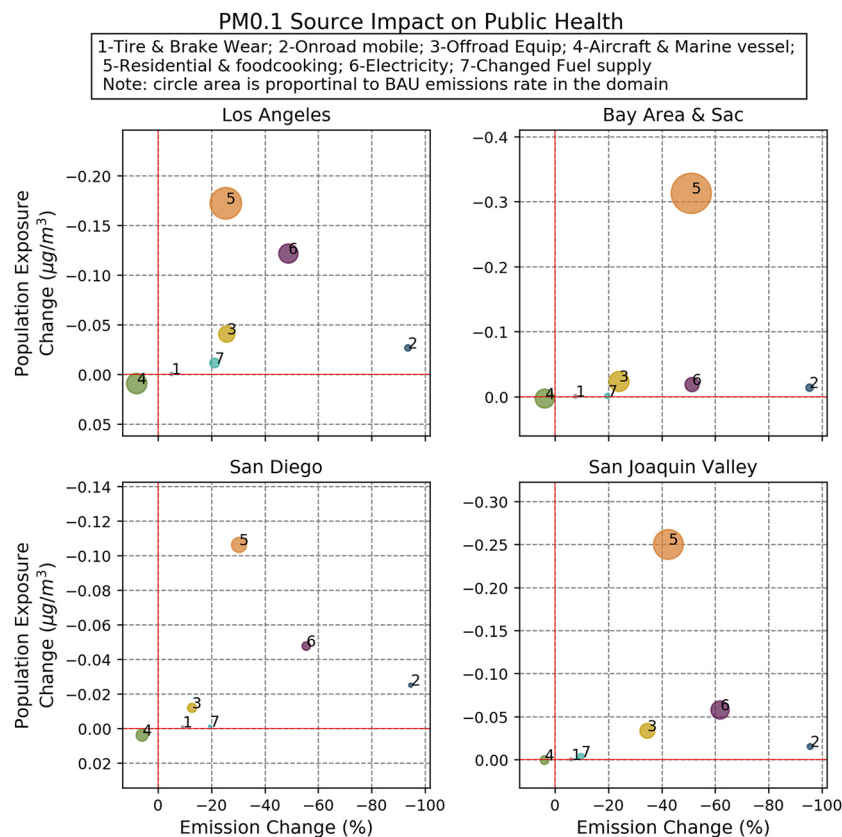


**Fig. 8.** PM<sub>0.1</sub> source impact on public health (regardless of race) for GHGAI energy scenario. X-axis indicates emissions (source) changes between BAU and GHGAI scenario. Y-axis indicates PWC changes between BAU and GHGAI scenario for specific source. All results averaged across four meteorological scenarios.

disproportionately affect groups with the highest exposure concentrations. Fig. 9 illustrates the emissions reduction for each source category in the GHGAI scenario relative to the BAU scenario along with the corresponding reduction in absolute disparity. Plots for other energy scenarios are shown in Figs. S41–S48. Ideal emissions sectors for further reductions are represented as large circles in the upper left quadrant of each plot. Large residential and food cooking emissions are a promising sector for further emissions reductions across all regions since each unit of emissions reduction produces a significant reduction in disparity. Further reductions in electricity generation emissions would reduce disparity in LA, but would have lower impact in other regions. Fig. 10 identifies candidate emissions sectors that could be targeted to reduce  $PM_{0.1}$  exposure disparities. Large emissions from residential and food cooking and electricity generation contribute strongly to  $PM_{0.1}$  exposure disparities across all regions. These sources could be targeted in future efforts to reduce  $PM_{0.1}$  exposure disparities.

### 3.5.3. Balancing benefits for total population and reduced disparity

The ideal future energy scenario will reduce exposure for the total population while simultaneously reducing exposure disparity between race/ethnicity groups. Fig. 11 illustrates how changes in the GHGAI scenario relative to the BAU scenario affected total population exposure to  $PM_{2.5}$  and the absolute exposure disparity. Fig. 12 illustrates the same plot for  $PM_{0.1}$

concentrations. Results for other scenarios are shown in Figs. S49–S56. All points in the upper right quadrant of each sub-panel indicate beneficial reductions in both disparity and total population exposure. Points below the 1:1 line (45° angle) reduce disparity by a larger amount than they reduce total population exposure. All points in Figs. 11 and 12 generally fall above the 1:1 line, indicating that statewide adoption of low carbon energy sources reduces total population exposure by an amount that is greater than or equal to the corresponding reduction in exposure disparities between racial groups. This finding suggests that statewide energy policies are not the ideal tool to reduce exposure disparities across race/ethnicity categories. Additional emissions controls may need to be applied in targeted neighborhoods to eliminate exposure disparity.

## 4. Conclusions

Total population exposure to  $PM_{2.5}$  and  $PM_{0.1}$  in California decreased when GHG mitigation strategies using low-carbon fuels or carbon-capture and sequestration were adopted compared to a Business as Usual (BAU) scenario in the year 2050. The relative pattern of air pollution exposure for different GHG mitigation strategies scenarios was consistent across the four meteorology scenarios considered in the present analysis. The greatest exposure reduction occurred under the deepest GHG reduction scenario (GHGAI), closely followed by two scenarios with slightly higher exposure

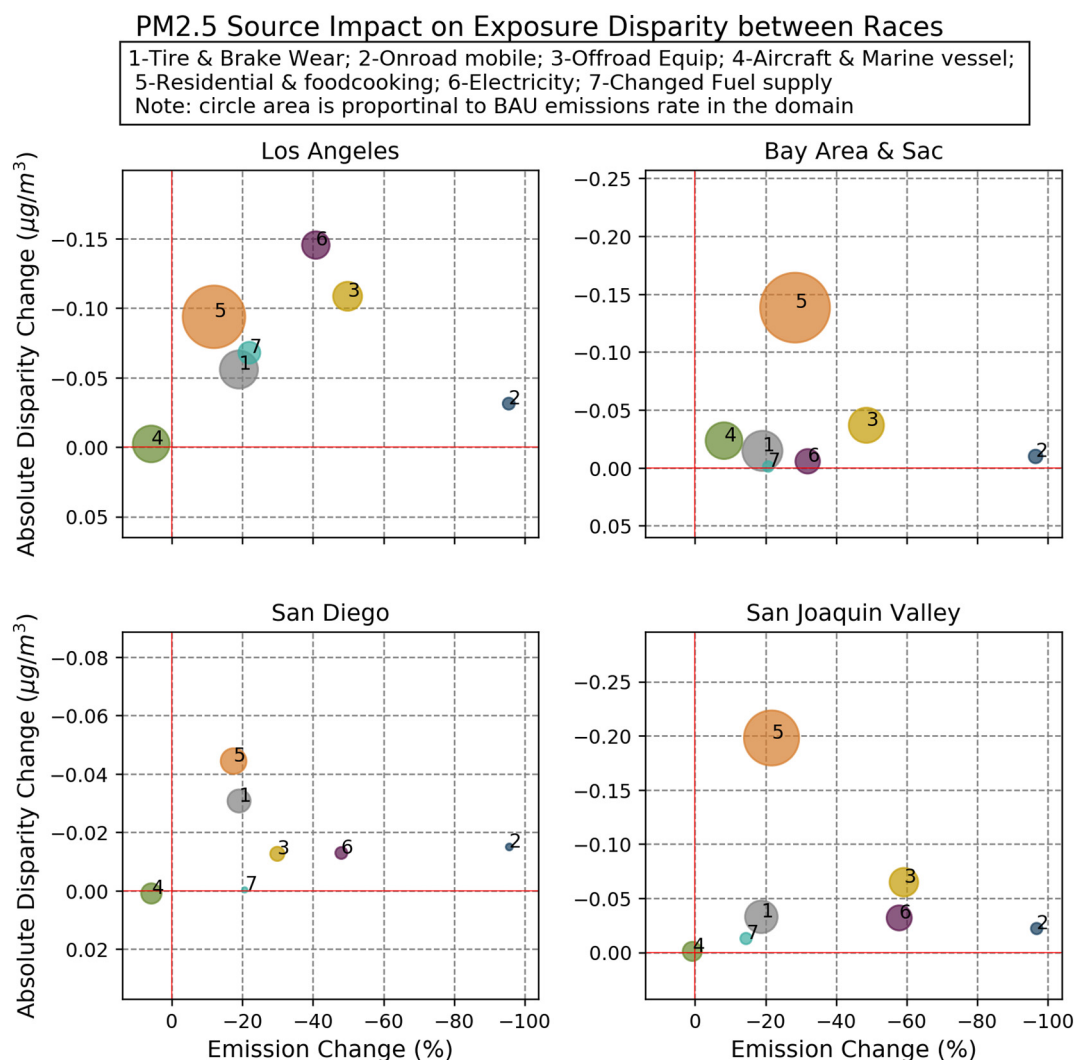
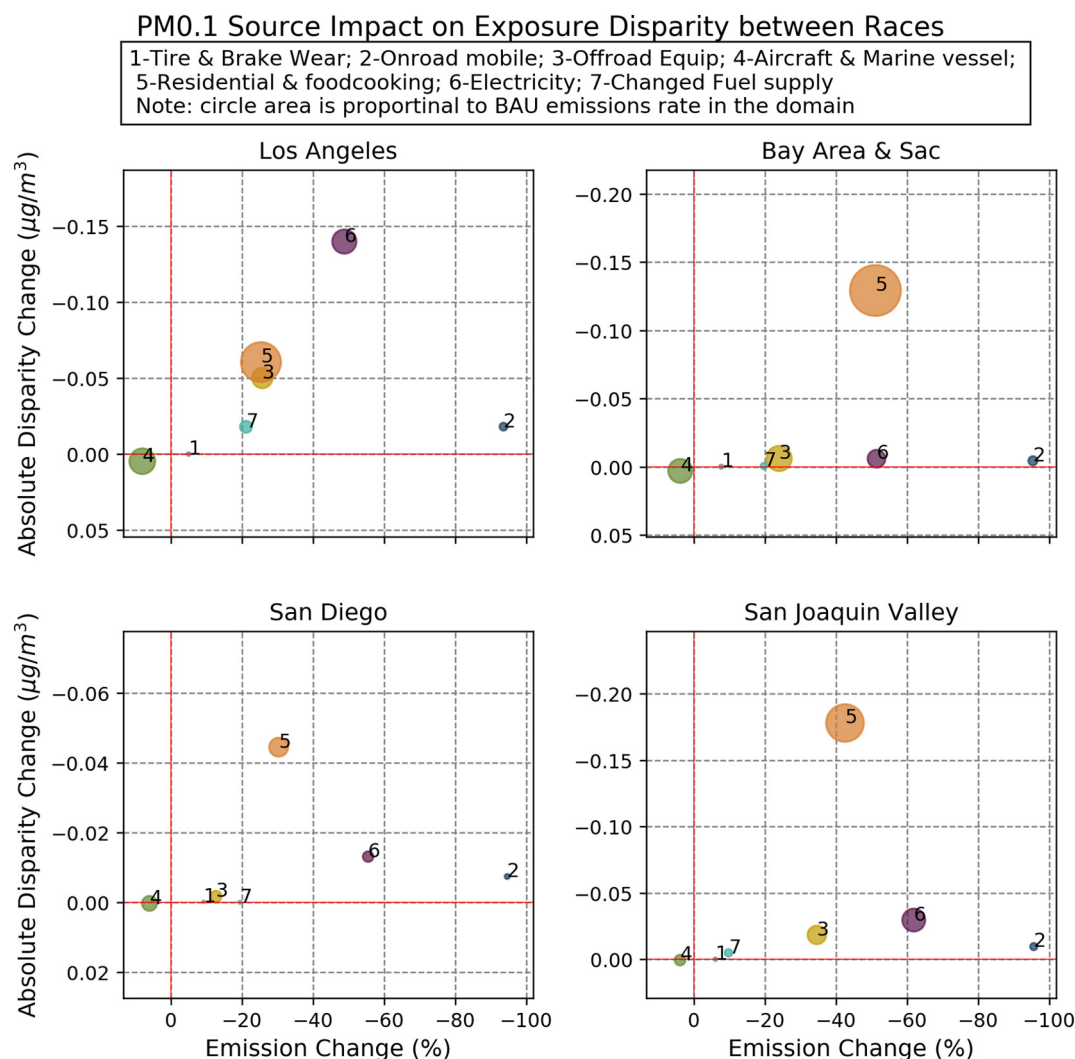


Fig. 9.  $PM_{2.5}$  source impact on exposure disparity between races for GHGAI energy scenario. X-axis indicates emissions (source) changes between BAU and GHGAI scenario. Y-axis indicates emission absolute disparity changes between BAU and GHGAI scenario for specific source. All results averaged across four meteorological scenarios.



**Fig. 10.** PM<sub>0.1</sub> source impact on exposure disparity between races for GHGAI energy scenario. X-axis indicates emissions (source) changes between BAU and GHGAI scenario. Y-axis indicates emission absolute disparity changes between BAU and GHGAI scenario for specific source. All results averaged across four meteorological scenarios.

due to increased natural gas utilization (NGB and NGT). Population-weighted PM<sub>2.5</sub> exposure averaged across all energy scenarios ranged from 8.2 µg/m<sup>3</sup> to 12.5 µg/m<sup>3</sup> depending on the region (LA, SD, SFBA & SAC, SJV), while PM<sub>0.1</sub> exposure ranged from 1.3 µg/m<sup>3</sup> to 2.2 µg/m<sup>3</sup>. Within the same region, relative reductions in PM<sub>0.1</sub> concentrations due to the adoption of low-carbon energy were up to four times larger than relative reductions in PM<sub>2.5</sub> concentrations (10–12% reduction for PM<sub>0.1</sub> vs. 2.5–2.7% reduction for PM<sub>2.5</sub>).

Trends in PM<sub>2.5</sub> and PM<sub>0.1</sub> absolute exposure disparity between race/ethnicity groups under different energy scenarios were similar to trends in total population exposure. Deep GHG reduction scenarios, including GHGAI, NGT, and NGB, produced the greatest reduction in absolute exposure disparity for PM<sub>2.5</sub> and PM<sub>0.1</sub>. None of the clean energy scenarios completely eliminated air pollution exposure disparity in the future, but adoption of low-carbon-energy sources did reduce the race/ethnicity disparity in California by as much as 20% for PM<sub>2.5</sub> mass and by as much as 40% for PM<sub>0.1</sub> mass.

Black & African American residents experienced higher-than-average exposure to PM<sub>2.5</sub> and PM<sub>0.1</sub> in all future energy scenarios in all study regions (LA, SD, SFBA & SAC, SJV). Asian residents in San Francisco experienced higher-than-average exposure to air pollution in all future energy scenarios. Peak exposure disparities reached ~10% above the average for PM<sub>2.5</sub> and ~20% above the average for PM<sub>0.1</sub>. White residents in all regions

experienced lower-than-average exposures in all energy scenarios, with peak disparity values of approximately –10% below the average for both PM<sub>2.5</sub> and PM<sub>0.1</sub>. Health co-benefits calculations predict that adoption lower carbon energy scenarios (GHGAI, NGT, NGB) produce greater public health saving for all races/ethnicities. Health benefits per 1 M residents are similar for Asian and Black & African American residents, slightly lower for Hispanic residents, and slightly higher for White residents.

The pattern of exposure disparities identified in the current study reflects the geographical distribution of each race/ethnicity group relative to the urban cores of each study city. Black & African American residents in California are more likely to live in urban cores or near major transportation corridors/industrial facilities where air pollution emissions are higher. In contrast, White residents are more dispersed in suburban areas that are further away from concentrated emissions sources. Additional emissions controls at the regional or local level will be needed to address these location-based disparities. Future demographic changes associated with population aging and population migration could either reduce or increase the need for additional emissions controls depending on how those changes affect the clustering of race/ethnicity groups towards urban cores.

Three source categories were identified for potential additional controls to further reduce PM<sub>2.5</sub>/PM<sub>0.1</sub> exposure disparities: i) residential heating &

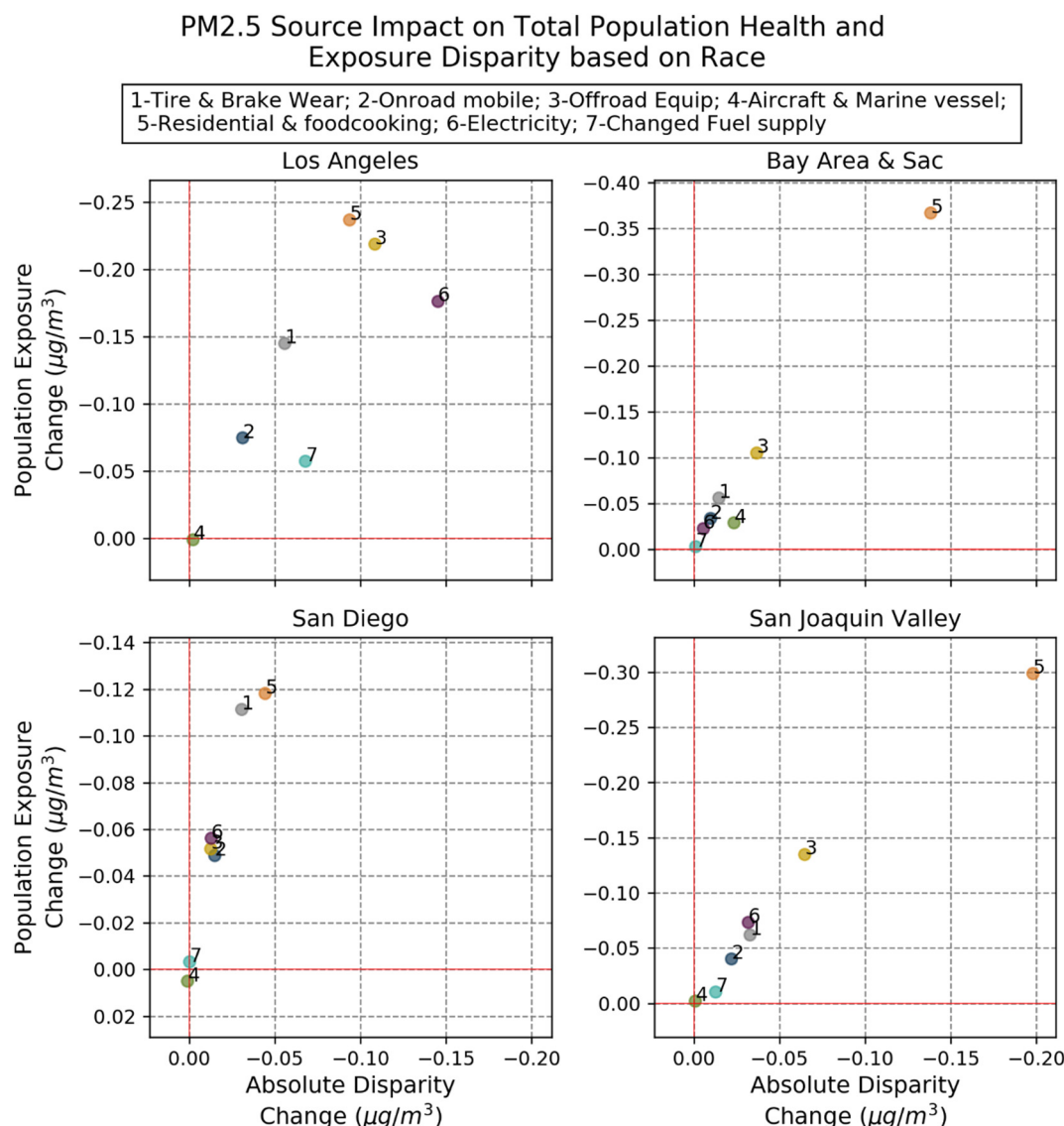


**Fig. 11.** PM<sub>2.5</sub> source impact on total population exposure and exposure disparity based on race for GHGAI energy scenario. X-axis indicates largest disparity changes between BAU and GHGAI scenario for each specific source. Y-axis indicates PWC changes between BAU and GHGAI scenario for each specific source. All results averaged across four meteorological scenarios.

food cooking, ii) tire and brake wear emissions, and iii) electricity generation. Local or regional emissions controls that target these categories could include the adoption electric heating to replace biomass combustion and natural gas combustion, modification of commercial cooking methods to reduce smoke emissions, increased use of regenerative braking to reduce brake emissions, development of new tire compounds to reduce tire wear emissions, and selective upgrading of electrical generating equipment to solar/wind/geothermal/hydro sources with battery backup. Future studies should consider the cost-effectiveness of each additional measure to create an optimized strategy to reduce PM<sub>2.5</sub>/PM<sub>0.1</sub> exposure disparities in California.

#### CRedit authorship contribution statement

Yiting Li developed methodology, performed the formal analysis, and wrote the original draft of the manuscript. Anikender Kumar performed formal analysis. Yin Li performed formal analysis. Michael Kleeman acquired funding, administered the project, developed methodology, developed software, and revised the manuscript.

#### Declaration of competing interest

The authors declare the following financial interests/personal relationships which may be considered as potential competing interests: Michael Kleeman reports financial support was provided by US Environmental Protection Agency.

#### Acknowledgements

This research was funded by the United States Environmental Protection Agency under Grant No. R83587901. Although the research described in the article has been funded by the United States Environmental Protection Agency it has not been subject to the Agency's required peer and policy review and therefore does not necessarily reflect the reviews of the Agency and no official endorsement should be inferred.

#### Appendix A. Supplementary data

Supplementary data to this article can be found online at <https://doi.org/10.1016/j.scitotenv.2022.155230>.

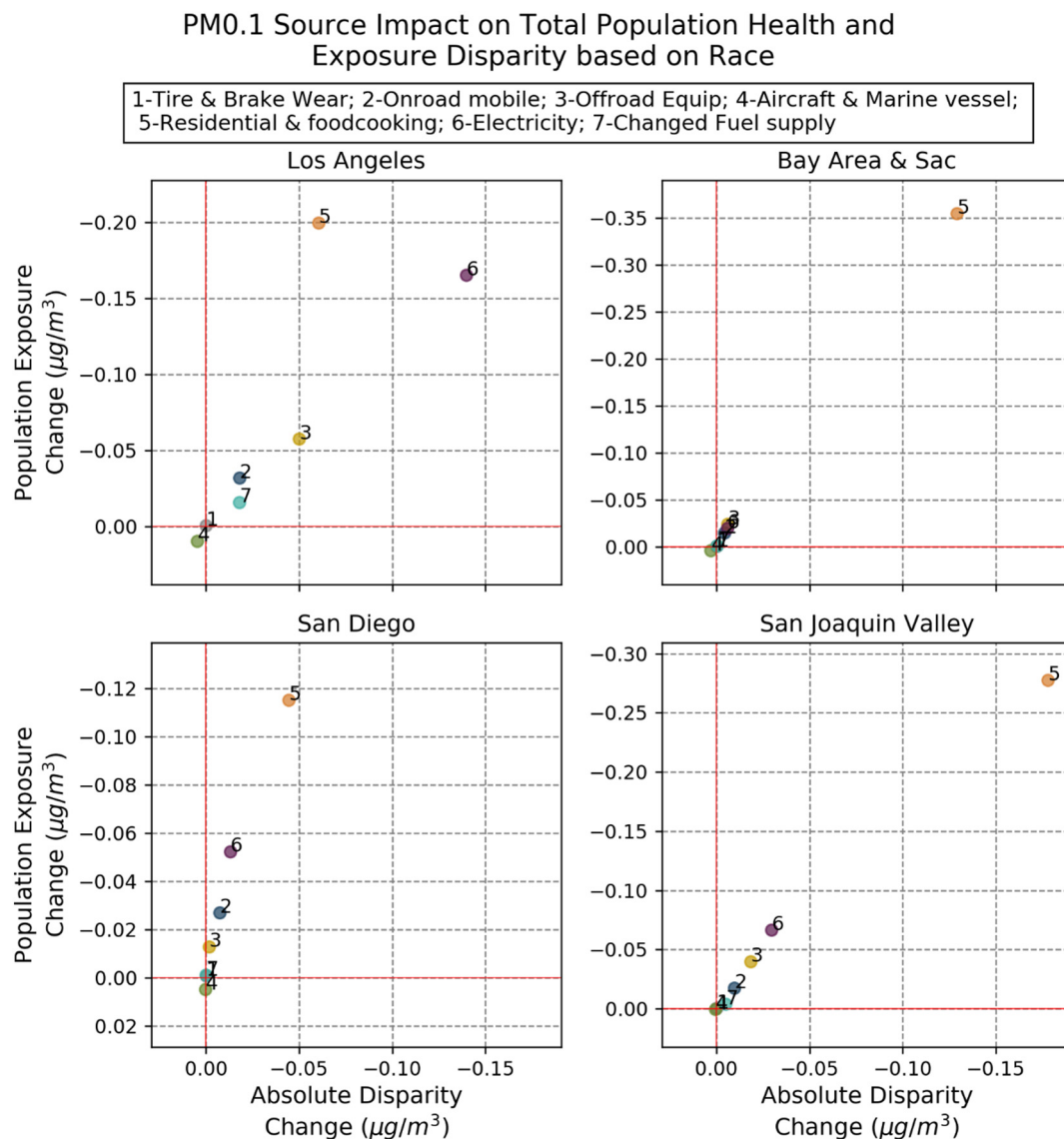


**Fig. 12.** PM<sub>0.1</sub> source impact on total population exposure and exposure disparity based on race for GHGAi energy scenario. X-axis indicates largest disparity changes between BAU and GHGAi scenario for each specific source. Y-axis indicates PWC changes between BAU and GHGAi scenario for each specific source. All results averaged over four meteorological scenarios.

## References

- American Lung Association, 2019. State of the Air 2019. [online] Available from <https://www.stateoftheair.org/assets/sota-2019-full.pdf>. (Accessed 26 December 2020).
- Anderson, C.M., Kissel, K.A., Field, C.B., Mach, K.J., 2018. Climate change mitigation, air pollution, and environmental justice in California. *Environ. Sci. Technol.* 52 (18), 10829–10838. <https://doi.org/10.1021/acs.est.8b00908>.
- Bravo, M.A., Anthopolos, R., Bell, M.L., Miranda, M.L., 2016. Racial isolation and exposure to airborne particulate matter and ozone in understudied US populations: environmental justice applications of downscaled numerical model output. *Environ. Int.* 92–93, 247–255. <https://doi.org/10.1016/j.envint.2016.04.008>.
- Cai, R., Zhao, C., Nie, X., 2019. Alumina-based coating with dimples as enabling sustainable technology to reduce wear and emission of the brake system. *ACS Sustain. Chem. Eng.* 8 (2), 893–899. <https://doi.org/10.1021/ACSUSCHEMENG.9B05302>.
- California Air Resource Board, 2006. Assembly Bill No. 32: Air Pollution: Greenhouse gases: California Global Warming Solutions Act of 2006. [online] Available from [https://leginfo.ca.gov/faces/billTextClient.xhtml?bill\\_id=200520060AB32](https://leginfo.ca.gov/faces/billTextClient.xhtml?bill_id=200520060AB32). (Accessed 26 July 2021).
- Cappa, C.D., Jathar, S.H., Kleeman, M.J., Docherty, K.S., Jimenez, J.L., Seinfeld, J.H., Wexler, A.S., 2016. Simulating secondary organic aerosol in a regional air quality model using the statistical oxidation model - part 2: assessing the influence of vapor wall losses. *Atmos. Chem. Phys.* 16 (5), 3041–3059. <https://doi.org/10.5194/ACP-16-3041-2016>.
- Clark, L.P., Millet, D.B., Marshall, J.D., 2017. Changes in transportation-related air pollution exposures by race-ethnicity and socioeconomic status: outdoor nitrogen dioxide in the United States in 2000 and 2010. *Environ. Health Perspect.* 125 (9). <https://doi.org/10.1289/EHP959>.
- Organization, W.H., 2021. WHO Global Air Quality Guidelines: Particulate Matter (PM<sub>2.5</sub> And PM<sub>10</sub>), Ozone, Nitrogen Dioxide, Sulfur Dioxide And Carbon Monoxide. World Health Organization.
- Colmer, J., Hardman, I., Shimshack, J., Voorheis, J., 2020. Disparities in PM<sub>2.5</sub> air pollution in the United States. *Science* (80-) 369 (6503), 575–578. <https://doi.org/10.1126/SCIENCE.AAZ9353>.
- Cushing, L., Faust, J., August, L.M., Cendak, R., Wieland, W., Alexeeff, G., 2015. Racial/ethnic disparities in cumulative environmental health impacts in California: evidence from a statewide environmental justice screening tool (CalEnviroScreen 1.1). *Am. J. Public Health* 105 (11), 2341–2348. <https://doi.org/10.2105/AJPH.2015.302643>.
- Dalmiau, M.E., Augsbury, K., Wenzel, F., Ivanov, V., 2020. Tire particle emissions: demand on reliable characterization. *Tire Sci. Technol.* 48 (2), 107–122. <https://doi.org/10.2346/TIRE.19.170181>.
- Dimanchev, E.G., Paltsev, S., Yuan, M., Rothenberg, D., Tessum, C.W., Marshall, J.D., Selin, N.E., 2019. Health co-benefits of sub-national renewable energy policy in the US. *Environ. Res. Lett.* 14 (8), 085012. <https://doi.org/10.1088/1748-9326/AB31D9>.
- Driscoll, C.T., Buonocore, J.J., Levy, J.I., Lambert, K.F., Burtraw, D., Reid, S.B., Fakhraei, H., Schwartz, J., 2015. US power plant carbon standards and clean air and health co-benefits. *Nat. Clim. Chang.* 5 (6), 535–540. <https://doi.org/10.1038/nclimate2598>.
- Evans, J.S., Wolff, S.K., Phonboon, K., Levy, J.I., Smith, K.R., 2002. Exposure efficiency: an idea whose time has come? *Chemosphere* 49 (9), 1075–1091. [https://doi.org/10.1016/S0045-6535\(02\)00242-4](https://doi.org/10.1016/S0045-6535(02)00242-4).
- Fonseca, G., Rodrigues, C., Oliveira, N.P., Rodrigues, G.F.C., Oliveira, N.P., Filho, W.L., De, J.B.S., Guerra, A., 2020. Impacts of green tire technology: case study of environmental

- and customer perspectives. *Clim. Chang. Manag.* 271–285. [https://doi.org/10.1007/978-3-030-57235-8\\_21](https://doi.org/10.1007/978-3-030-57235-8_21).
- Fountoukis, C., Nenes, A., 2007. *Atmospheric Chemistry and Physics ISORROPIA II: a computationally efficient thermodynamic equilibrium model for K + Ca 2 + Mg 2 + NH 4 + Na + SO 2 - 4 NO - 3 Cl - H 2 O aerosols*. *Atmos. Chem. Phys.* 7, 4639–4659 [online]. Available from: [www.atmos-chem-phys.net/7/4639/2007/](http://www.atmos-chem-phys.net/7/4639/2007/) (Accessed 14 February 2022).
- Gent, P., Donner, L., Lawrence, D., Gent, P.R., Danabasoglu, G., Donner, L.J., Holland, M.M., Hunke, E.C., Jayne, S.R., Lawrence, D.M., Neale, R.B., Rasch, P.J., Vertenstein, M., Worley, P.H., Yang, Z.-L., Zhang, M., 2011. The Community Climate System Model Version 4 OCEANFILMS View project Dust Emission Modeling View project The Community Climate System Model Version 4. *Artic. J. Clim.* <https://doi.org/10.1175/2011JCLI4083.1>.
- Gov Arnold Schwarzenegger, C., 2005. *Executive Order S-3-05*.
- Gramstad, S., 2018. Technological measures for brake wear emission reduction: possible improvement in compositions and technological remediation: cost efficiency. *Non-Exhaust Emiss.* 205–227. <https://doi.org/10.1016/B978-0-12-811770-5.00010-8>.
- Gunier, R.B., Hertz, A., Von Behren, J., Reynolds, P., 2003. Traffic density in California: socio-economic and ethnic differences among potentially exposed children. *J. Expo. Anal. Environ. Epidemiol.* 13 (3), 240–246. <https://doi.org/10.1038/sj.eja.7500276>.
- Harper, S., Ruder, E., Roman, H.A., Geggel, A., Nweke, O., Payne-Sturges, D., Levy, J.I., 2013. Using inequality measures to incorporate environmental justice into regulatory analyses. *Int. J. Environ. Res. Public Health* 10 (9), 4039–4059. <https://doi.org/10.3390/ijerph100904039>.
- Houston, D., Li, W., Wu, J., 2014. Disparities in exposure to automobile and truck traffic and vehicle emissions near the Los Angeles-long beach port complex. *Am. J. Public Health* 104 (1), 156–164. <https://doi.org/10.2105/AJPH.2012.301120>.
- Hu, J., Zhang, H., Chen, S.-H., Wiedinmyer, C., Vandenberghe, F., Ying, Q., Kleeman, M.J., 2014. Predicting primary PM<sub>2.5</sub> and PM<sub>0.1</sub> trace composition for epidemiological studies in California. *Environ. Sci. Technol.* 48, 4971–4979. <https://doi.org/10.1021/es404809j>.
- Hu, J., Zhang, H., Ying, Q., Chen, S.-H., Vandenberghe, F., Kleeman, M.J., 2015. Long-term particulate matter modeling for health effect studies in California – part 1: model performance on temporal and spatial variations. *Atmos. Chem. Phys.* 15, 3445–3461. <https://doi.org/10.5194/acp-15-3445-2015>.
- Hu, J., Jathar, S., Zhang, H., Ying, Q., Chen, S.-H., Cappa, C.D., Kleeman, M.J., 2017. Long-term particulate matter modeling for health effect studies in California – part 2: concentrations and sources of ultrafine organic aerosols. *Atmos. Chem. Phys.* 17, 5379–5391. <https://doi.org/10.5194/acp-17-5379-2017>.
- Jacobson, M.Z., 2010. A solution to the problem of nonequilibrium acid/base gas-particle transfer at long time step. 39(2), pp. 92–103. <https://doi.org/10.1080/027868290904546>.
- Karner, A.A., Eisinger, D.S., Niemeier, D.A., 2010. Near-roadway air quality: synthesizing the findings from real-world data. *Environ. Sci. Technol.* 44, 5334–5344. <https://doi.org/10.1021/es100008x>.
- Kleeman, M.J., Cass, G.R., 2001. A 3D Eulerian source-oriented model for an externally mixed aerosol. *Environ. Sci. Technol.* 35 (24), 4834–4848. <https://doi.org/10.1021/es010886m>.
- Kleeman, M.J., Zapata, C., Stille, J., Hixson, M., 2013. PM<sub>2.5</sub> co-benefits of climate change legislation part 2: California governor's executive order S-3-05 applied to the transportation sector. *Clim. Chang.* 117, 399–414. <https://doi.org/10.1007/s10584-012-0546-x>.
- Krewski, D., Jerrett, M., Burnett, R.T., Ma, R., Hughes, E., Shi, Y., Turner, M.C., Newbold, B., Ramsay, T., Ross, Z., Shin, H., Tempalski, B., 2009. *Extended follow-up and spatial analysis of the American Cancer Society study linking particulate air pollution and mortality*. *Am. J. Respir. Crit. Care Med.* 173 (6), 667–672. <https://doi.org/10.1164/RCCM.200503-443OC>.
- Laurent, O., Hu, J., Li, L., Cockburn, M., Escobedo, L., Kleeman, M.J., Wu, J., 2014. Sources and contents of air pollution affecting term low birth weight in Los Angeles County, California, 2001–2008. *Environ. Res.* 134, 488–495. <https://doi.org/10.1016/j.envres.2014.05.003>.
- Lelieveld, J., Evans, J.S., Fnais, M., Giannadaki, D., Pozzer, A., 2015. The contribution of outdoor air pollution sources to premature mortality on a global scale. *Nature* 525 (7569), 367–371. <https://doi.org/10.1038/nature15371>.
- Lepeule, J., Laden, F., Dockery, D., Schwartz, J., 2012. Chronic exposure to fine particles and mortality: an extended follow-up of the Harvard six cities study from 1974 to 2009. *Environ. Health Perspect.* 120 (7), 965. <https://doi.org/10.1289/EHP.1104660>.
- Levy, J.I., Woo, M.K., Penn, S.L., Omari, M., Tambouret, Y., Kim, C.S., Arunachalam, S., 2016. Carbon reductions and health co-benefits from US residential energy efficiency measures. *Environ. Res. Lett.* 11 (3), 034017. <https://doi.org/10.1088/1748-9326/11/3/034017>.
- Li, Y., Rodier, C., Lea, J.D., Harvey, J., Kleeman, M.J., 2020. Improving spatial surrogates for area source emissions inventories in California. *Atmos. Environ.* 117665. <https://doi.org/10.1016/j.atmosenv.2020.117665>.
- Li, Y., Yang, C., Li, Y., Kumar, A., Kleeman, M.J., 2022. Future emissions of particles and gases that cause regional air pollution in California under different greenhouse gas mitigation strategies. *Atmos. Environ.* 273, 118960. <https://doi.org/10.1016/J.ATMOSENV.2022.118960>.
- Liu, J., Clark, L.P., Bechle, M.J., Hajat, A., Kim, S.Y., Robinson, A.L., Sheppard, L., Szpiro, A.A., Marshall, J.D., 2021. Disparities in air pollution exposure in the United States by race/ethnicity and income, 1990–2010. *Environ. Health Perspect.* 129 (12). <https://doi.org/10.1289/EHP8584> undefined-undefined.
- Mahmud, A., Hixson, M., Kleeman, M.J., 2012. Atmospheric chemistry and physics quantifying population exposure to airborne particulate matter during extreme events in California due to climate change. *Atmos. Chem. Phys.* 12, 7453–7463. <https://doi.org/10.5194/acp-12-7453-2012>.
- Markandya, A., Sampedro, J., Smith, S.J., Van Dingenen, R., Pizarro-Irizar, C., Arto, I., González-Eguino, M., 2018. Health co-benefits from air pollution and mitigation costs of the Paris Agreement: a modelling study. *Lancet Planet. Health* 2 (3), e126–e133. [https://doi.org/10.1016/S2542-5196\(18\)30029-9](https://doi.org/10.1016/S2542-5196(18)30029-9).
- Marshall, J.D., Riley, W.J., McKone, T.E., Nazaroff, W.W., 2003. Intake fraction of primary pollutants: motor vehicle emissions in the South Coast Air Basin. *Atmos. Environ.* 37 (24), 3455–3468. [https://doi.org/10.1016/S1352-2310\(03\)00269-3](https://doi.org/10.1016/S1352-2310(03)00269-3).
- Marshall, J.D., Teoh, S.K., Nazaroff, W., 2005. Intake fraction of nonreactive vehicle emissions in US urban areas. *Atmos. Environ.* 39 (7), 1363–1371. <https://doi.org/10.1016/J.ATMOSENV.2004.11.008>.
- McCollum, D., Yang, C., Yeh, S., Ogden, J., 2012. Deep greenhouse gas reduction scenarios for California – strategic implications from the CA-TIMES energy-economic systems model. *Energy Strateg. Rev.* 1, 19–32. <https://doi.org/10.1016/j.esr.2011.12.003>.
- Miranda, M.L., Edwards, S.E., Keating, M.H., Paul, C.J., 2011. Making the environmental justice grade: the relative burden of air pollution exposure in the United States. *Int. J. Environ. Res. Public Health* 8 (6), 1755–1771. <https://doi.org/10.3390/ijerph8061755>.
- NACR, 2012. User's Guide for the Advanced Research WRF (ARW) Modeling System Version 3.4.ite. [online]. Available from [https://www2.mmm.ucar.edu/wrf/users/docs/user\\_guide\\_V3.4/user\\_guide\\_V3.4/contents.html](https://www2.mmm.ucar.edu/wrf/users/docs/user_guide_V3.4/user_guide_V3.4/contents.html).
- Nardone, A., Chiang, J., Corburn, J., 2020. Historic redlining and urban health today in U.S. cities. [online]. Available from *Environ. Justice* 13 (4), 109–119. [https://doi.org/10.1089/ENV.2020.0011/ASSET/IMAGES/LARGE/ENV.2020.0011\\_FIGURE3.JPEG](https://doi.org/10.1089/ENV.2020.0011/ASSET/IMAGES/LARGE/ENV.2020.0011_FIGURE3.JPEG).
- Ostro, B., Hu, J., Goldberg, D., Reynolds, P., Hertz, A., Bernstein, L., Kleeman, M.J., 2015. Associations of mortality with long-term exposures to fine and ultrafine particles, species and sources: results from the California teachers study cohort. *Environ. Health Perspect.* 123, 549–556. <https://doi.org/10.1289/ehp.1408565>.
- Panko, J., Kreider, M., Unice, K., 2018. Review of tire wear emissions: a review of tire emission measurement studies: identification of gaps and future needs. *Non-Exhaust Emiss.* 147–160. <https://doi.org/10.1016/B978-0-12-811770-5.00007-8>.
- Paoletta, D.A., Tessum, C.W., Adams, P.J., Apte, J.S., Chambliss, S., Hill, J., Muller, N.Z., Marshall, J.D., 2018. Effect of model spatial resolution on estimates of fine particulate matter exposure and exposure disparities in the United States. *Environ. Sci. Technol. Lett.* 5 (7), 436–441. <https://doi.org/10.1021/acs.estlett.8b00279>.
- Perlin, S.A., Setzer, R.W., Creason, J., Sexton, K., 2002. Distribution of industrial air emissions by income and race in the United States: an approach using the toxic release inventory. *Environ. Sci. Technol.* 29 (1), 69–80. <https://doi.org/10.1021/ES00001A008>.
- Pope, C.A., Burnett, R.T., Thun, M.J., Calle, E.E., Krewski, D., Ito, K., Thurston, G.D., 2002. Lung cancer, cardiopulmonary mortality, and long-term exposure to fine particulate air pollution. *JAMA* 287 (9), 1132–1141. <https://doi.org/10.1001/JAMA.287.9.1132>.
- Ramaswami, A., Tong, K., Fang, A., Lal, R.M., Nagpure, A.S., Li, Y., Yu, H., Jiang, D., Russell, A.G., Shi, L., Chertow, M., Wang, Y., Wang, S., 2017. Urban cross-sector actions for carbon mitigation with local health co-benefits in China. *Nat. Clim. Chang.* (10), 736–742. <https://doi.org/10.1038/ndclimate3373>.
- Rowangould, G.M., 2013. A census of the US near-roadway population: public health and environmental justice considerations. *Transp. Res. D Transp. Environ.* 25, 59–67. <https://doi.org/10.1016/J.TRD.2013.08.003>.
- Sampedro, J., Smith, S.J., Arto, I., González-Eguino, M., Markandya, A., Mulvaney, K.M., Pizarro-Irizar, C., Van Dingenen, R., 2020. Health co-benefits and mitigation costs as per the Paris Agreement under different technological pathways for energy supply. *Environ. Int.* 136, 105513. <https://doi.org/10.1016/J.ENVINT.2020.105513>.
- Shah, R.U., Robinson, E.S., Gu, P., Apte, J.S., Marshall, J.D., Robinson, A.L., Presto, A.A., 2020. Socio-economic disparities in exposure to urban restaurant emissions are larger than for traffic. *Environ. Res. Lett.* <https://doi.org/10.1088/1748-9326/abc92>.
- Strak, M., Weinmayr, G., Rodopoulou, S., Chen, J., De Hoogh, K., Andersen, Z.J., Atkinson, R., Bauerle, M., Bekkevold, T., Bellander, T., Bouton-Ruault, M.C., Brandt, J., Cesaroni, G., Concin, H., Fehst, D., Forastiere, F., Gulliver, J., Hertel, O., Hoffmann, B., Hvidtfeldt, U.A., Janssen, N.A.H., Jöckel, K.H., Jørgensen, J.T., Ketzel, M., Klompaker, J.O., Lager, A., Leander, K., Liu, S., Ljungman, P., Magnusson, P.K.E., Mehta, A.J., Nagel, G., Ofstedal, B., Pershagen, G., Peters, A., Raaschou-Nielsen, O., Renzi, M., Rizzato, D., Van Der Schouw, Y.T., Schramm, S., Severi, G., Sigsgaard, T., Sørensen, M., Stafoggia, M., Tjønneland, A., Monique Verschuren, W., Vienneau, D., Wolf, K., Katsouyanni, K., Brunekreef, B., Hoek, G., Samoli, E., 2021. Long term exposure to low level air pollution and mortality in eight European cohorts within the ELAPSE project: pooled analysis. *BMJ* 374. <https://doi.org/10.1136/BMJ.N1904>.
- Swart, N.C., Cole, J.N.S., Kharin, V.V., Lazare, M., Scinocca, J.F., Gillett, N.P., Anstey, J., Arora, V., Christian, J.R., Hanna, S., Jiao, Y., Lee, W.G., Majaess, F., Saenko, O.A., Seiler, C., Seinen, C., Shao, A., Sigmund, M., Solheim, L., Von Salzen, K., Yang, D., Winter, B., 2019. The Canadian Earth System Model Version 5 (CanESM5.0.3). *Geosci. Model Dev.* 12 (11), 4823–4873. <https://doi.org/10.5194/GMD-12-4823-2019>.
- Tessum, C.W., Apte, J.S., Goodkind, A.L., Muller, N.Z., Mullins, K.A., Paoletta, D.A., Polasky, S., Springer, N.P., Thakrar, S.K., Marshall, J.D., Hill, J.D., 2019. Inequity in consumption of goods and services adds to racial-ethnic disparities in air pollution exposure. *Proc. Natl. Acad. Sci. U. S. A.* <https://doi.org/10.1073/pnas.1818859116>.
- Tessum, C.W., Paoletta, D.A., Chambliss, S.E., Apte, J.S., Hill, J.D., Marshall, J.D., 2021. PM<sub>2.5</sub> pollutants disproportionately and systemically affect people of color in the United States. *Sci. Adv.* 7 (18), 4491–4519. <https://doi.org/10.1126/sciadv.abf4491>.
- Thakrar, S.K., Balasubramanian, S., Adams, P.J., Azevedo, M.L., Muller, N.Z., Pandis, S.N., Polasky, S., Arden, C., Robinson, A.L., Apte, J.S., Tessum, C.W., Marshall, J.D., Hill, J.D., 2020. Reducing mortality from air pollution in the United States by targeting specific emission sources. *Cite This Environ. Sci. Technol. Lett.* 7, 639–645. <https://doi.org/10.1021/acs.estlett.0c00424>.
- Thind, M.P.S., Tessum, C.W., Azevedo, I.L., Marshall, J.D., 2019. Fine particulate air pollution from electricity generation in the US: health impacts by race, income, and geography. *Environ. Sci. Technol.* 53 (23), 14010–14019. <https://doi.org/10.1021/ACS.EST.9B02527>.

- United State Census Bureau, 2020. American Community Survey (ACS) data. [online] Available from [https://www2.census.gov/geo/tiger/TIGER\\_DP/](https://www2.census.gov/geo/tiger/TIGER_DP/). (Accessed 14 December 2020).
- US EPA, 2021. Technical Support Document (TSD) for the final revised cross-state air pollution rule update for the 2008 ozone season NAAQS. [online] Available from [https://www.epa.gov/sites/default/files/2021-03/documents/estimating\\_pm2.5\\_and\\_ozone-attributable\\_health\\_benefits\\_tsd\\_march\\_2021.pdf](https://www.epa.gov/sites/default/files/2021-03/documents/estimating_pm2.5_and_ozone-attributable_health_benefits_tsd_march_2021.pdf).
- Wang, T., Jiang, Z., Zhao, B., Gu, Y., Liou, K.N., Kalandiyur, N., Zhang, D., Zhu, Y., 2020. Health co-benefits of achieving sustainable net-zero greenhouse gas emissions in California. *Nat. Sustain.* 3 (8), 597–605. <https://doi.org/10.1038/s41893-020-0520-y>.
- West, J.J., Fiore, A.M., Horowitz, L.W., Mauzerall, D.L., 2017. Global health benefits of mitigating ozone pollution with methane emission controls. *Proc. Natl. Acad. Sci. U. S. A.* 114, 3988–3993. <https://doi.org/10.1073/pnas.0600201103>.
- Yang, C., Yeh, S., Zakerinia, S., Ramea, K., McCollum, D., 2015. Achieving California's 80% greenhouse gas reduction target in 2050: technology, policy and scenario analysis using CA-TIMES energy economic systems model. *Energy Policy* 77.
- Ying, Q., Fraser, M.P., Griffin, R.J., Chen, J., Kleeman, M.J., 2007. Verification of a source-oriented externally mixed air quality model during a severe photochemical smog episode. *Atmos. Environ.* 41.
- Yu, X., Venecek, M., Kumar, A., Hu, J., Tanrikulu, S., Soon, S.T., Tran, C., Fairley, D., Kleeman, M.J., 2019. Regional sources of airborne ultrafine particle number and mass concentrations in California. *Atmos. Chem. Phys.* 19 (23), 14677–14702. <https://doi.org/10.5194/ACP-19-14677-2019>.
- Zapata, C.B., Yang, C., Yeh, S., Ogden, J., Kleeman, M.J., 2018a. Estimating criteria pollutant emissions using the California Regional Multisector Air Quality Emissions (CA-RE-MARQUE) model v1.0. *Geosci. Model Dev.* 11, 1293–1320. <https://doi.org/10.5194/gmd-11-1293-2018>.
- Zapata, C.B., Yang, C., Yeh, S., Ogden, J., Kleeman, M.J., 2018b. Low-carbon energy generates public health savings in California. *Atmos. Chem. Phys.* 18, 4817–4830. <https://doi.org/10.5194/acp-18-4817-2018>.
- Zenou, Y., Boccard, N., 2000. Racial discrimination and redlining in cities. *J. Urban Econ.* 48 (2), 260–285. <https://doi.org/10.1006/JUEC.1999.2166>.
- Zhang, Y., Bowden, J.H., Adelman, Z., Naik, V., Horowitz, L.W., Smith, S.J., West, J.J., 2016. Co-benefits of global and regional greenhouse gas mitigation for US air quality in 2050. *Atmos. Chem. Phys.* 16 (15), 9533–9548. <https://doi.org/10.5194/acp-16-9533-2016>.
- Zhang, Y., Smith, S.J., Bowden, J.H., Adelman, Z., West, J.J., 2017. Co-benefits of global, domestic, and sectoral greenhouse gas mitigation for US air quality and human health in 2050. *Environ. Res. Lett.* 12 (11). <https://doi.org/10.1088/1748-9326/aa8f76>.
- Zhao, B., Wang, T., Jiang, Z., Gu, Y., Liou, K.N., Kalandiyur, N., Gao, Y., Zhu, Y., 2019. Air quality and health cobenefits of different deep decarbonization pathways in California. *Environ. Sci. Technol.* 53 (12), 7163–7171. <https://doi.org/10.1021/acs.est.9b02385>.